Optical Engineering

OpticalEngineering.SPIEDigitalLibrary.org

Rayleigh Brillouin optical time-domain analysis system using heterodyne detection and wavelength scanning

Yongqian Li
Lixin Zhang
Hanbai Fan
Hong Li

SPIE.

Yongqian Li, Lixin Zhang, Hanbai Fan, Hong Li, "Rayleigh Brillouin optical time-domain analysis system using heterodyne detection and wavelength scanning," *Opt. Eng.* **57**(5), 056112 (2018), doi: 10.1117/1.OE.57.5.056112.

Rayleigh Brillouin optical time-domain analysis system using heterodyne detection and wavelength scanning

Yongqian Li, Lixin Zhang,* Hanbai Fan, and Hong Li
North China Electric Power University, Department of Electronics and Communication Engineering, Baoding, China

Abstract. This study proposes the use of heterodyne detection and wavelength scanning techniques to solve the problems of small signal and large noise in a Rayleigh Brillouin optical time-domain analysis (BOTDA) system and thereby improve the system performance. Based on an analysis of the Rayleigh BOTDA system, heterodyne detection is used to enhance the signal intensity and wavelength scanning is used to reduce the fading noise. Experimental results obtained using the proposed techniques show that the amplitude fluctuation and signal-to-noise ratio in a 50-m-long fiber near the fiber end with 17 wavelength scans-based averaging are, respectively, reduced by 0.91 dB and increased by 4.19 dB compared to those with a single wavelength. Furthermore, the Brillouin frequency shift in a 70-m-long fiber heated to 50°C and inserted at the center of the sensing fiber can be measured accurately with a maximum fluctuation of 0.19 MHz; this is equivalent to a temperature measurement accuracy of 0.19°C. These results indicate that the proposed techniques can realize high-accuracy measurement, and therefore, they show great potential in the field of long-distance and high-accuracy sensing. [DOI: 10.1117/1.OE.57.5.056112]

Keywords: Brillouin optical time-domain analysis; nondestructive measurement; wavelength scanning; heterodyne detection; fading noise; Rayleigh scattering.

Paper 172074 received Jan. 5, 2018; accepted for publication May 14, 2018; published online May 30, 2018.

1 Introduction

Distributed fiber optic sensors based on Brillouin optical time-domain analysis (BOTDA) have been used widely for structural health monitoring (SHM) of large-scale civil infrastructure because they enable the distributed monitoring of temperature or strain in kilometer-long fibers with submeter resolution.[1–2] In a traditional BOTDA system, a pump wave and a probe wave propagate in opposite directions along the optical fiber. When the probe wave lies within the Brillouin spectrum of the pump wave, stimulated Brillouin scattering (SBS) interaction occurs, and the probe wave experiences an amplification or attenuation depending on whether its frequency is lower or higher than that of the pump wave. Although traditional BOTDA systems afford advantages such as high signal-to-noise ratio (SNR) and long sensing distance, the requirement of a two-ended structure makes them inconvenient for large-scale SHM applications, such as monitoring the operating condition of a power cable with very long transmission distance, or applications in which the signal will become unavailable if the fiber is broken.

To improve the applicability of BOTDA systems, in 1996, Nikles et al.[3] proposed a single-ended structure that uses the Fresnel reflection of the sensing fiber end as a probe wave. Subsequently, some similar configurations were proposed and demonstrated experimentally to enhance the performance of Fresnel-reflection-based single-ended BOTDA systems.[4–6] However, Fresnel reflection at the fiber end is directly related to the condition of the fiber end face, for example, how clean it is or whether it has a connector; the condition strongly influences the measurement. Therefore, a single-ended BOTDA system that uses Fresnel reflection of the fiber end can only achieve limited performance.

In 2011, Cui et al.[7] demonstrated a single-ended direct-detection BOTDA temperature sensing system in which Rayleigh backscattering in the fiber is used as the probe light. A Rayleigh BOTDA system can be operated even if the sensing fiber is broken and is not affected by the condition of the fiber end face; therefore, it affords unique advantages such as nondestructive measurement, single light source, and single-ended operation. However, a Rayleigh BOTDA system has a much smaller probe light than a traditional BOTDA system; this leads to a small signal and low SNR in the system. Among various system noises, coherent fading noise is dominant; it is generated by the phase correlation between Rayleigh backscattered lights. Therefore, it is essentially a signal-induced noise and cannot be effectively reduced by the commonly used signal averaging approach. As a result, it causes nonegligible amplitude fluctuations in the backscattered trace. On the other hand, as the wavelength scanning of a laser source can change the relative phase relations between the Rayleigh backscattered lights, if numerous independent backscattered signals measured at different frequencies are averaged, then the phase correlations between Rayleigh backscattered lights and thus the coherent fading noise can be reduced greatly. Although wavelength-scanning-based signal averaging techniques have been successfully used in coherent optical time-domain reflectometry and coherent optical frequency-domain reflectometry[8–12] for characterization and fault location in an optical fiber transmission system, few studies have focused on Brillouin distributed sensing.[13]

*Address all correspondence to: Lixin Zhang, E-mail: zhanglxmail@126.com

In this paper, we propose a Rayleigh BOTDA system with improved SNR in which heterodyne detection and wavelength scanning techniques are used to enhance the signal intensity and to reduce the coherent fading noise, respectively. The principle analysis of signal intensity enhancement and amplitude fluctuation reduction in the proposed system is conducted theoretically, and an experimental setup is constructed to realize Rayleigh-BOTDA-based temperature sensing using the proposed techniques. Finally, the performances of the Rayleigh BOTDA temperature sensing system with single wavelength and 17 wavelength scans-based averaging are discussed based on a comparison of the experimental results.

2 Theory

2.1 *Principle of Heterodyne Detection Rayleigh BOTDA System*

Figure 1 shows a schematic of the heterodyne detection Rayleigh BOTDA system. Synthetic light composed of a continuous Stokes light and a pulsed light enters the sensing fiber. Then, the Rayleigh backscattering produced by continuous Stokes light acts as a probe light, and the pulsed light acts as a pump light for SBS interaction with the probe light. The probe light frequency v_R is down-shifted from the pump light frequency v_P by v_m that is tunable in the vicinity of Brillouin frequency shift (BFS) v_B of the fiber. When the probe light falls into the Brillouin gain spectrum of the pump light, SBS interaction occurs, and therefore, the probe light experiences an SBS gain in the sensing fiber. The SBS interaction becomes the maximum when the optical frequency difference between the probe light and the pump light is equal to the BFS. Heterodyne detection for measuring the Brillouin gain spectrum can be realized by introducing a coherent local light that is mixed up with the backscattered probe light on a photodetector (PD) at the input end.

If the difference between the local light frequency v_L and probe light frequency v_R is v_f, then the probe light carrying the SBS information and local light can be represented as

$$E_R(t) = E_R \cos[2\pi v_R t + \varphi_R(t)] H_{SBS}(\nu, z), \tag{1}$$

$$E_L(t) = E_L \cos[2\pi v_L t + \varphi_L(t)], \tag{2}$$

where E_R, v_R, and $\varphi_R(t)$ are, respectively, the probe light's optical field intensity, frequency, and phase at time t; $H_{SBS}(v, z)$ is the SBS transfer function; and E_L, $v_L = v_R - v_f$, and $\varphi_L(t)$ are the local light's optical field intensity, frequency, and phase, respectively.

For local heterodyne detection, the ac component of the photocurrent from the PD in the heterodyne detection Rayleigh BOTDA system can be expressed as

$$\begin{aligned} i_{ac} &\propto R[E_R(t) + E_L(t)][\overline{E}_R(t) + \overline{E}_L(t)] \\ &\propto R\sqrt{P_R P_L} H_{SBS}(\nu, z) \cos\theta(t) \cos[2\pi v_f t + \varphi_R(t) - \varphi_L(t)], \end{aligned} \tag{3}$$

where R is the responsivity of the PD, – is the conjugate, $\theta(t)$ is the relative polarization angle between the probe light and the local light, and P_R and P_L are the powers of the probe light and local light, respectively.

Equation (3) shows that after heterodyne detection, the probe light is amplified by a factor of $\sqrt{P_L}$ and the heterodyne signal frequency is decided only by v_f. Therefore, the amplitude and frequency stability of the achieved signal can be improved by selecting a local light with suitably higher power and a v_f signal generator with high-frequency stability.

2.2 *Method for Reducing Fading Noise*

In a heterodyne detection Rayleigh BOTDA system, amplitude fluctuations of the detected heterodyne signal are mostly caused by the coherent fading noises resulting from the interference between the Rayleigh backscattered lights in the fiber, variation of the relative phase, and polarization angle between the Rayleigh backscattered signal and the local light in the PD, as given in Eq. (3). The amplitude fluctuations generated by the polarization variation in the Rayleigh backscattered signal and local light can be reduced by carefully controlling the polarization of the continuous Stokes light and pulsed pump light using polarization controllers (PCs) and adequately scrambling the polarizations of the Rayleigh backscattered signal and local light using polarization scramblers (PSs); as a result, the influence of polarization variation in the Rayleigh BOTDA system can be neglected.

Coherent Rayleigh noise (CRN) results from the interference among numerous lightwaves backscattered at different

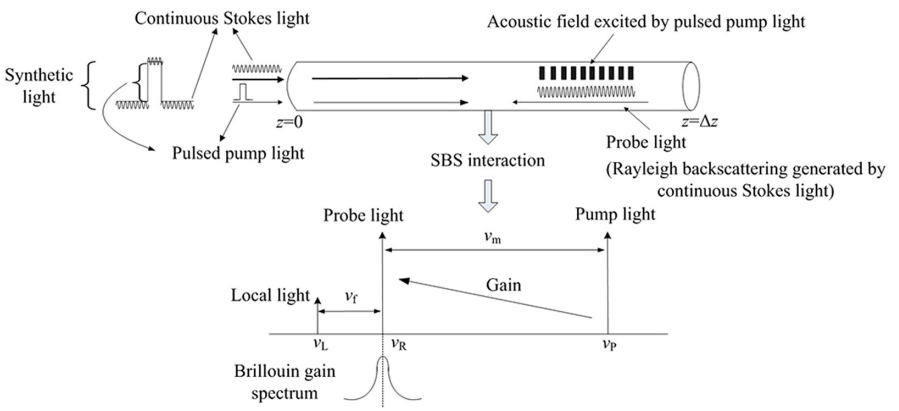

Fig. 1 Schematic diagram of heterodyne detection Rayleigh BOTDA system.

locations in the fiber through phase-intensity conversion, and it manifests as temporal amplitude fluctuations in the Rayleigh backscattered signal trace.[10] Because the CRN is signal-induced, it is amplified together with the probe light when SBS gain occurs, and thus, CRN becomes more severe in a Rayleigh BOTDA system. This reduces the SNR of the system and imposes a serious limitation on the achievable measurement accuracy. On the other hand, from the property of CRN, it can be known that if the wavelength of the laser source and physical state of the sensing fiber remain constant during the measurement time of Rayleigh BOTDA system, then the CRN-induced amplitude fluctuations in the Rayleigh signal should remain invariant. Furthermore, if the wavelength of the laser source is changed, then the relative phase relations of the Rayleigh backscattered lights also change, indicating that the phase correlation between the Rayleigh backscattered lights can be reduced effectively by wavelength scanning. As a result, by averaging the measured independent backscattered signals at different frequencies with changed relative phase relations and reduced phase correlations after wavelength scanning, the CRN-induced amplitude fluctuation can be reduced greatly.

Assuming that the frequency of the laser source is changed from F_0 to $F_0 + F$, where F_0 is the laser frequency without wavelength scanning and F is the frequency scanning range, the frequency interval of wavelength scanning is given as

$$\Delta F = F/n, \tag{4}$$

where n is the number of wavelength scans. The correlative range in which strong correlation is maintained and the correlative period are, respectively, expressed as[9]

$$l_{\min} = V_g/4F, \tag{5}$$

$$l_{\text{cycle}} = V_g/4\Delta F = V_g n/4F, \tag{6}$$

where V_g is the group velocity of light in the fiber.

Furthermore, assuming that N, $\Delta z/l_{\min}$, is the number of correlative scatter elements within the spatial resolution range Δz without scanning the laser wavelength; M, $1 + \Delta z/l_{\text{cycle}}$, is the number of scatter elements among which strong phase correlations still remain after wavelength scanning; and the number of phase correlative scatter elements is reduced from N to M by wavelength scanning, the reduction of correlative scatter elements through wavelength scanning can be given by the ratio

$$\frac{M}{N} = \frac{V_g}{4\Delta z F}\left(1 + \frac{4\Delta z F}{n V_g}\right). \tag{7}$$

The square root of the variance of the Rayleigh backscattering intensity can be considered as the amplitude fluctuation with respect to its mean value due to coherent fading noise. Therefore, the relative amplitude fluctuation of the detected probe light in units of dB is given as[10]

$$\Delta = 5\ \log(\langle I\rangle + \sigma) - 5\ \log(\langle I\rangle) = 5\ \log[1 + \sigma/\langle I\rangle], \tag{8}$$

where $\langle I\rangle$ is the mean value of the detected probe light intensity I, and σ is the square root of the variance of I.

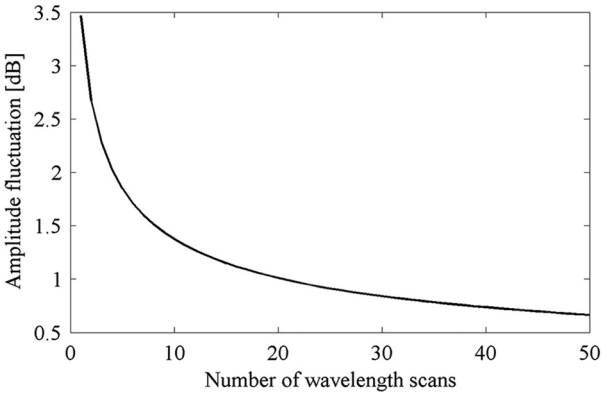

Fig. 2 Amplitude fluctuation versus number of wavelength scans.

Thus, the relative amplitude fluctuation of the detected probe light is given as

$$\Delta = 5\ \log[1 + (\langle I^2\rangle - \langle I\rangle^2)^{1/2}/\langle I\rangle]. \tag{9}$$

Because the number of phase correlative scatter elements is reduced from N to M after wavelength scanning, the variance of the detected probe light intensity $\langle I^2\rangle - \langle I\rangle^2$ can be replaced by $(M/N)\langle I\rangle^2$.[9] Upon substituting the variance of intensity I into Eq. (9), the amplitude fluctuation is given as

$$\Delta = 5\ \log[1 + (M/N)^{1/2}] = 5\ \log\left[1 + \left(\frac{V_g}{4\Delta z F} + \frac{1}{n}\right)^{1/2}\right]. \tag{10}$$

Equation (10) shows that the amplitude fluctuation can be reduced by increasing the frequency scanning range and scanning number. More specifically, when $\Delta z F$ is kept constant, with an increase in the wavelength scanning number, the amplitude fluctuation first decreases rapidly and then decreases slowly to a stable value, as is shown in Fig. 2. As show in Fig. 2, the simulation parameters, $V_g = 2 \times 10^8$ m/s, $\Delta z = 13$ m, and $F = 20$ GHz, have been used. Similarly, according to Eq. (10), when n is kept constant, the amplitude fluctuation shows a similar trend with an increase in the frequency scanning range. Furthermore, the characteristics of CRN-induced amplitude fluctuation shown in Eq. (10) can be well understood as follows: when the period of correlation becomes larger than the spatial resolution owing to a much larger number of scans in a specific frequency range, there will be no correlation scatter elements over Δz, and therefore, the amplitude fluctuation becomes stable.

3 Experimental Details

Figure 3 shows the experimental setup for a heterodyne detection Rayleigh BOTDA sensing system using wavelength scanning. A tunable laser with a linewidth of ~100 Hz and an output power of 16 dBm operates in the wavelength range of 1549.66 to 1549.82 nm. The laser output is divided into two branches by a 20:80 polarization-maintaining coupler (PMC). The upper branch with 20% output is modulated into the pulsed pump light using electrooptic modulator 1 (EOM1) with a high extinction ratio of 40 dB; EOM1 is driven by a pulse generator. After being amplified by Erbium-doped fiber amplifier 1 (EDFA1), the pump pulses

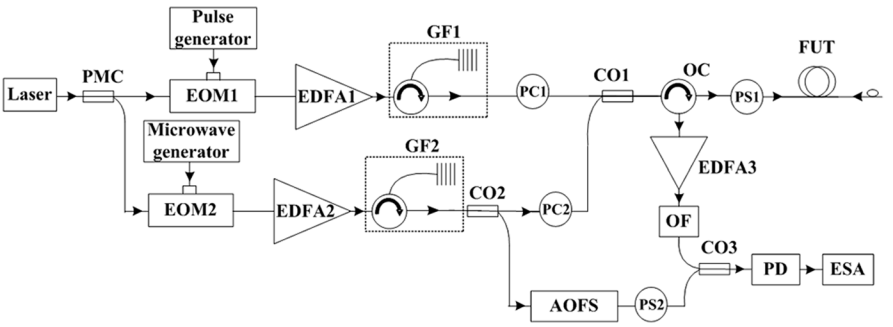

Fig. 3 Experimental setup for heterodyne detection Rayleigh BOTDA sensing system using wavelength scanning.

are directed to Bragg grating filter 1 (GF1) with a central wavelength of 1549.686 nm and a bandwidth of 0.236 nm to filter out the amplified spontaneous emission noise (ASEN). The lower branch with 80% output is modulated into two sidebands, namely, the continuous Stokes and the anti-Stokes light, using EOM2 that is operated in the suppressed carrier regime and driven by a microwave generator with tunable frequency in the vicinity of BFS of the fiber under test (FUT). Similarly, after being amplified by EDFA2, the two modulated sidebands are passed through GF2 with a central wavelength of 1549.889 nm and a bandwidth of 0.35 nm to filter out the continuous anti-Stokes light and ASEN. The PC1 and PC2 inserted into the two branches are used to adjust the polarizations of the pulsed pump light and continuous Stokes light, respectively, to ensure the minimum polarization mismatch when the pulsed pump light and continuous Stokes light enter optical coupler 1 (CO1). Then, the synthetic light composed of the pulsed pump light and continuous Stokes light is transmitted into the FUT through an optical circulator (OC) and is scrambled by PS1 to reduce the polarization fading of SBS. The continuous Stokes light in the lower branch is split into two parts by CO2: the upper part is connected with CO1 through PC2, and the lower part is used to generate the local light through a 200-MHz downshifted acousto-optic frequency shifter (AOFS). The backscattered probe light carrying SBS information is amplified by EDFA3 to a desired power and is extracted by an optical filter (OF) with tunable central wavelength and bandwidth. Then, the backscattered probe light and local light are mixed together by CO_3 and detected by a 5 Hz to 1 GHz bandwidth PD. Before doing so, PS2 is used to scramble the polarization of local light to reduce the polarization fading caused by the polarization mismatch of the backscattered probe light and local light. Finally, a 13.6-GHz bandwidth electric spectrum analyzer (ESA) with an 8-MHz resolution bandwidth and operated in the "zero-span" mode is used to acquire the heterodyne detection amplitude traces along the sensing fiber at different beat frequencies.

In the experiment, the FUT is a standard single-mode communication fiber (SMF), G.652D, with a total length of ~1.97 km, and a knot is tied at the end of the fiber to minimize the impact of Fresnel reflection. Thereinto, the FUT is spliced into three sections with different lengths of 1 km, 70 m, and 900 m, respectively. The 70-m-long section is placed in a thermostatic water bath maintained at 50°C. At room temperature of 37.2°C, the BFSs of the three sections are measured to be ~10.850 GHz. The pulsed pump light has a width of 130 ns and a power of 23 dBm, and the powers of the continuous Stokes light and local light are set to be 6 and −10 dBm, respectively. The frequency of the microwave generator is changed from 10.800 to 10.910 GHz with a step of 5-MHz to cover the Brillouin spectrum of the FUT, and the sampled backscattered probe lights are averaged 5000 times to improve the SNR of the measurement.

4 Results and Discussions

In the experiment, the wavelength of the laser source is 1549.66 to 1549.82 nm, and it is adjusted in a step of 0.01 nm to obtain 17 backscattered signals at different wavelengths. To illustrate the performance improvement of the proposed system, the amplitude fluctuation reduction and temperature measurement accuracy enhancement are analyzed as follows.

4.1 *Amplitude Fluctuation Reduction*

As noted in Sec. 2.2, amplitude fluctuations are mostly caused by the coherent fading noise, including the amplitude fluctuation induced by the polarization variation of Rayleigh backscattering in the fiber and CRN-induced amplitude fluctuation. The obtained three-dimensional (3-D) amplitude spectrum with single wavelength and 17 wavelength scans in the heterodyne detection Rayleigh BOTDA system are shown in Fig. 4. It should be noted that for obtaining the 3-D amplitude spectrum with 17 wavelength scans, the detected 3-D amplitude spectra at different wavelengths are averaged. Figure 4 clearly shows that the amplitude fluctuation with single wavelength is much larger than that with 17 wavelength scans-based averaging. To further illustrate the decrease in amplitude fluctuation and increase in SNR upon performing wavelength scanning, the normalized amplitude distribution of the measured Brillouin time domain signals at the microwave generator frequency of 10.850 GHz with different numbers of wavelength scans is shown in Fig. 5.

From Fig. 5, it can be seen clearly that the amplitude fluctuation with single wavelength is obviously large, indicating that the CRN has a serious impact on the normalized Brillouin amplitude distribution. However, with an increase in the number of wavelength scans, the amplitude fluctuations gradually decreased, which demonstrates that the wavelength scanning can reduce the CRN effectively. And when the number of wavelength scans is smaller than some value, say 5, the amplitude fluctuation reduction is significant, but when the number of wavelength scans is larger than this

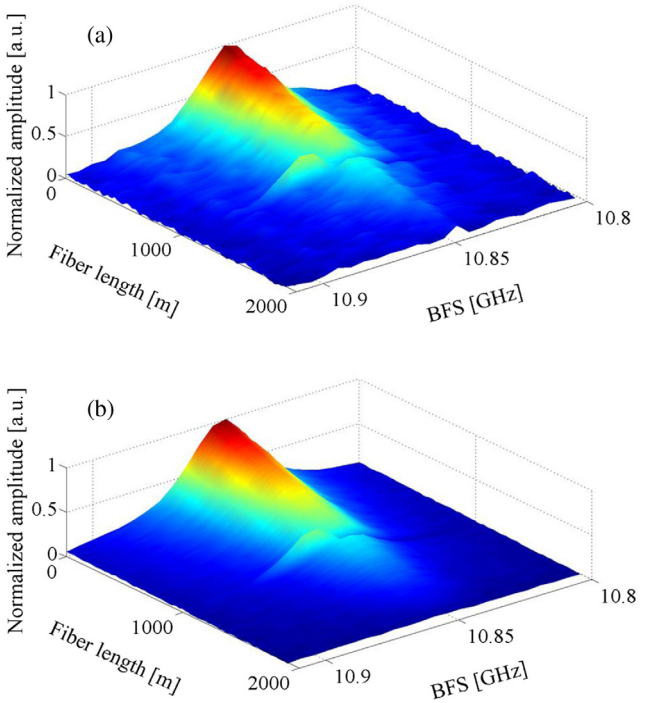

Fig. 4 3-D amplitude spectrum distribution in heterodyne detection Rayleigh BOTDA system (a) with single wavelength and (b) with 17 wavelength scans-based averaging.

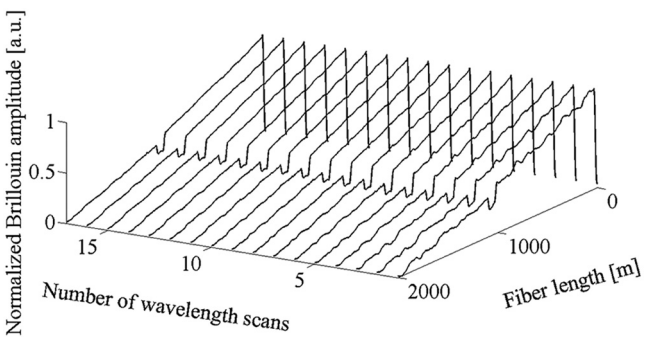

Fig. 5 Normalized Brillouin amplitude distribution along the sensing fiber in heterodyne detection Rayleigh BOTDA system with different numbers of wavelength scans.

value, the reduction of amplitude fluctuation is no longer obvious.

To quantitatively clarify the relationship between the amplitude fluctuation and the number of wavelength scans, the amplitude fluctuation of the measured Brillouin time domain signals at different wavelength is obtained by the linear fitting of the measurements at the frequency of 10.850 GHz to their mean value for the 50-m-long fiber near the fiber end. Figure 6 shows the amplitude fluctuation under n $(n = 1, \ldots, 17)$ wavelength scans-based averaging. This figure clearly shows that the amplitude fluctuation first decreases rapidly with an increase in the number of wavelength scans and then becomes stable for more than 8 wavelength scans; this is in good agreement with Eq. (10) and Fig. 2. Furthermore, calculations show that the maximum amplitude fluctuation with 17 wavelength scans is 0.913 dB smaller than that with single wavelength, and

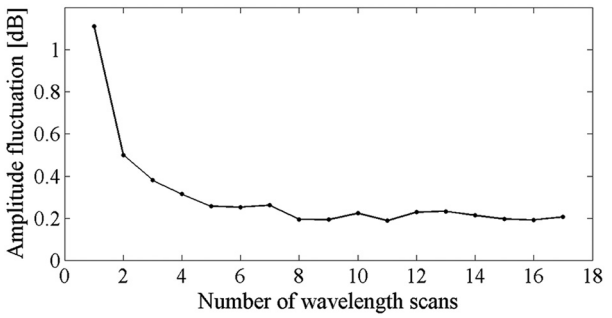

Fig. 6 Amplitude fluctuation versus number of wavelength scans n.

the root mean square errors with 17 wavelength scans-based averaging and single wavelength are 0.001834 and 0.004804, respectively. According to the SNR formula $R_{SN} = V^2/\sigma^2$ in which V is the signal voltage and σ is the standard deviation of noise, the SNR with 17 wavelength scans-based averaging is 4.19 dB higher than that with single wavelength, indicating that the sensing distance of the system can be increased using wavelength scanning.

To further demonstrate the effect of wavelength scanning in reducing the coherent fading noise, the amplitude fluctuation comparison between single wavelength with 17 measurements-based averaging, conducted in 17 h, and 17 wavelength scans-based averaging is given in Fig. 7. Through linear fitting of the measurements to their mean value in the 50-m-long fiber near the fiber end, the maximum Brillouin amplitude fluctuation under 17 wavelength

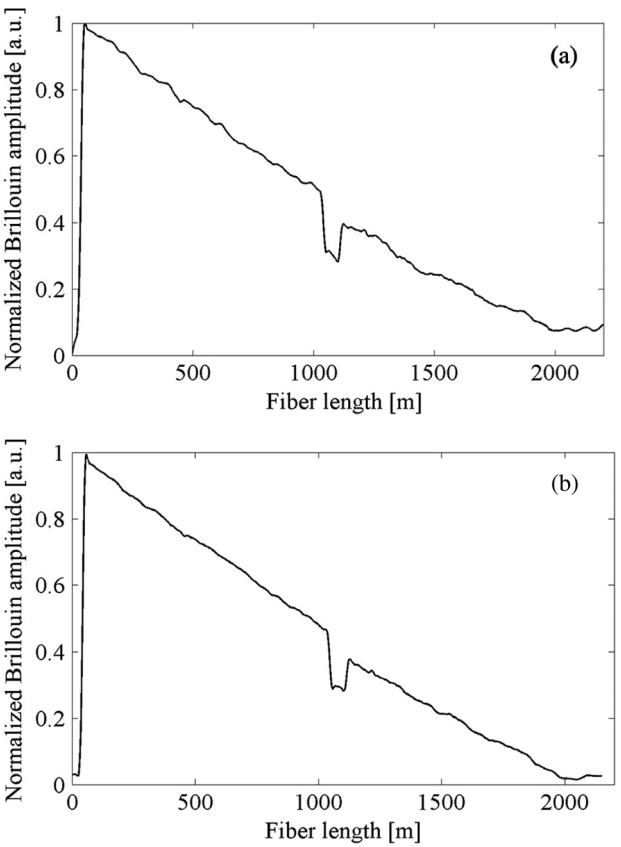

Fig. 7 Comparison of (a) single wavelength with 17 measurements-based averaging and (b) 17 wavelength scans-based averaging.

scans-based averaging and single wavelength with 17 measurements-based averaging are obtained to be 0.205 and 0.274 dB, respectively, which indicates that the wavelength scanning technique can reduce the coherent fading noise more effectively.

4.2 *Temperature Measurement Accuracy Improvement*

To estimate the temperature measurement accuracy of the proposed sensing system experimentally, the BFS distributions along the entire sensing fiber under single wavelength, single wavelength with 17 measurements-based averaging, and 17 wavelength scans-based averaging are acquired by fitting the measured spectra with Lorentzian curve, as shown in Fig. 8. From Fig. 8(a), it is clearly seen that the BFS shows an unmeasurable fluctuation near the fiber end in the single wavelength system and has a similar character even if the frequency fluctuation has been obviously reduced through 17 measurements-based averaging. By contrast, Fig. 8(c) shows that the BFS can be measured accurately with 17 wavelength scans-based averaging. Taking the maximum fluctuation of the BFS in the heated section as the temperature measurement accuracy, the temperature measurement accuracies under single wavelength, single wavelength with 17 measurements-based averaging, and 17 wavelength scans-based averaging are evaluated to be 4.17°C, 0.44°C, and 0.19°C because the frequency fluctuations in the 50-m-long fiber of the heated section are 4.17, 0.44, and 0.19 MHz, respectively.

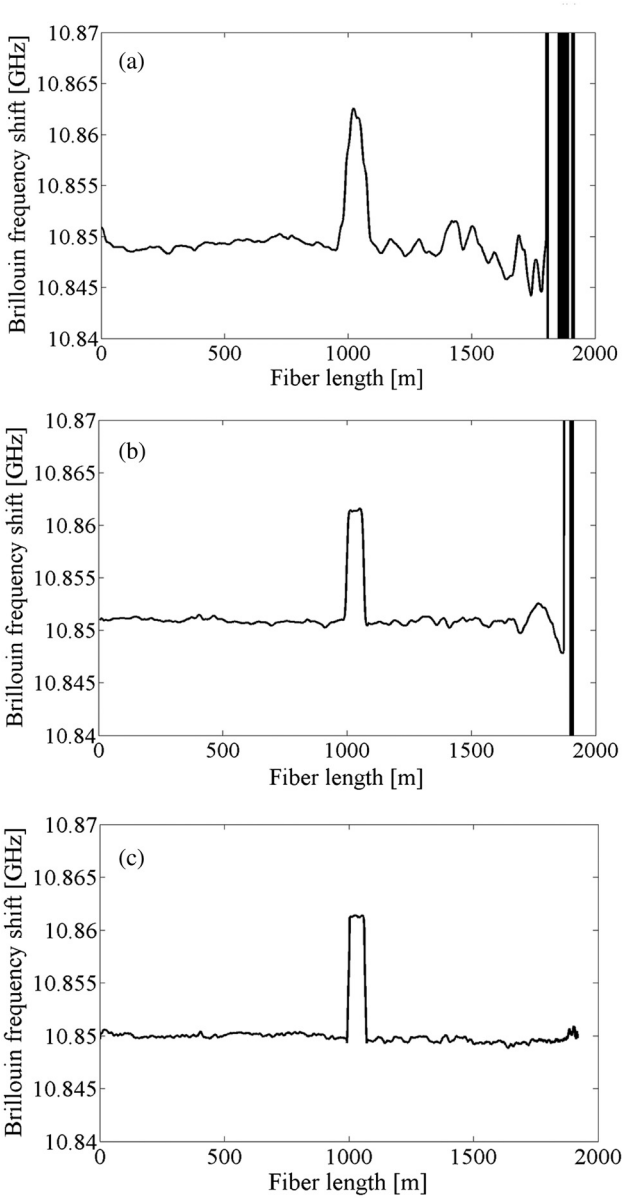

Fig. 8 BFS distribution along the sensing fiber in heterodyne detection Rayleigh BOTDA system under (a) single wavelength, (b) single wavelength with 17 measurements-based averaging, and (c) 17 wavelength scans-based averaging.

5 Conclusions

A Rayleigh BOTDA sensing system using heterodyne detection and wavelength scanning for enhancing the signal intensity and reducing the fading noise has been proposed and demonstrated theoretically and experimentally. We analyzed and compared the Brillouin amplitude and BFS distribution along the sensing fiber under different numbers of wavelength scans. The results show that the amplitude fluctuation and SNR for 17 wavelength scans-based averaging is reduced by 0.913 dB and enhanced by 4.19 dB, respectively, compared with those in a single wavelength system, and the BFS distribution along the sensing fiber can be measured accurately with 17 wavelength scans-based averaging. The analysis of the BFS fluctuation in the 50-m-long fiber of the heated section at the center of the 1.97-km-long sensing fiber shows that a temperature measurement accuracy of 0.19°C can be achieved with 17 wavelength scans-based averaging. These results indicate that the proposed techniques can effectively reduce the amplitude fluctuation and improve the SNR and temperature measurement accuracy in the Rayleigh BOTDA system. Therefore, the performance of single-ended distributed sensors can be improved, and new applications may be enabled.

Acknowledgments

This work was supported by the National Natural Science Foundation of China (NSFC) (Grant Nos. 61775057 and 61377088), the Natural Science Foundation of Hebei Province of China (Grant Nos. E2015502053 and F2015502059), and Fundamental Research Funds for the Central Universities (2016XS104).

References

1. X. Jia et al., "Frequency-comb-based BOTDA sensors for high-spatial-resolution/long-distance sensing," *Opt. Express* **25**(6), 6997–7007 (2017).
2. T. Kurashima, T. Horiguchi, and M. Tateda, "Distributed temperature sensing using stimulated Brillouin scattering in optical silica fibers," *Opt. Lett.* **15**(18), 1038–1040 (1990).
3. M. Nikles, L. Thevenaz, and P. Robert, "Simple distributed fiber sensor based on Brillouin gain spectrum analysis," *Opt. Lett.* **21**(10), 758–760 (1996).
4. Q. Cui et al., "Distributed fiber sensor based on modulated pulse base reflection and Brillouin gain spectrum analysis," *Appl. Opt.* **48**(30), 5823–5828 (2009).
5. X. Zhang, J. Hu, and Y. Zhang, "A hybrid single-end-access BOTDA and COTDR sensing system using heterodyne detection," *J. Lightwave Technol.* **31**(12), 1954–1959 (2013).
6. Z. Yang et al., "Single-ended distributed Brillouin sensing with high spatial resolution based on double-sideband long pulse," *Appl. Phys. Express* **6**(7), 072502 (2013).

7. Q. Cui et al., "Distributed temperature sensing system based on Rayleigh scattering BOTDA," *IEEE Sens. J.* **11**(2), 399–403 (2011).
8. H. Izumita et al., "Fading noise reduction in coherent OTDR," *IEEE Photonics Technol. Lett.* **4**(2), 201–203 (1992).
9. K. Shimizu, T. Horiguchi, and Y. Koyamada, "Characteristics and reduction of coherent fading noise in Rayleigh backscattering measurement for optical fibers and components," *J. Lightwave Technol.* **10**(7), 982–987 (1992).
10. H. Izumita et al., "Stochastic amplitude fluctuation in coherent OTDR and a new technique for its reduction by stimulating synchronous optical frequency hopping," *J. Lightwave Technol.* **15**(2), 267–278 (1997).
11. Z. He et al., "High-reflectivity-resolution coherent optical frequency domain reflectometry using optical frequency comb source and tunable delay line," *Opt. Express* **19**(26), B764–B769 (2011).
12. L. Lu et al., "Coherent optical time domain reflectometry by logarithmic detection and timed random frequency hopping," *Opt. Eng.* **56**(2), 024106 (2017).
13. K. De Souza, "Significance of coherent Rayleigh noise in fibre-optic distributed temperature sensing based on spontaneous Brillouin scattering," *Meas. Sci. Technol.* **17**(5), 1065–1069 (2006).

Yongqian Li received his BE degree in electronic instrument and measurement technology and his MS degree in communication and electronic system from Tianjin University, China, in 1982 and 1988, respectively. He received his PhD at Gunma University, Japan, in 2003. Since 2004, he has been a professor in the Department of Electronics and Communication Engineering, North China Electric Power University. His research interests include optical communication and distributed optical fiber sensing.

Lixin Zhang received her BE degree in electronic information science and technology from North China Electric Power University in 2011, and now she is a PhD student in North China Electric Power University with the major of electrical information technology. Her research interests include optical communication and distributed optical fiber sensing.

Hanbai Fan received his BE degree in Department of Electronics from Hebei University in 1988 and his MS degree in communications and information systems from North China Electric Power University. He is an associate professor in the Department of Electronics and Communication Engineering, North China Electric Power University. His research interests include the application of electronic technology, EDA technology, microcontroller, and embedded technology development and application areas.

Hong Li received her BE degree in electronic information science and technology from North China Electric Power University in 2016, and now she is a master student in North China Electric Power University with the major of electrical information technology. Her research interests include optical communication and distributed optical fiber sensing.